Journal of the Taiwan Institute of Chemical Engineers xxx (xxxx) xxx

Contents lists available at ScienceDirect

Journal of the Taiwan Institute of Chemical Engineers

journal homepage: www.elsevier.com/locate/jtice

Quantitative simultaneous determination of pentoxifylline and paracetamol in drug and biological samples at graphene nanoflakes modified electrode

S. Meenakshi [a,b], K. Pandian [a,*], S.C.B. Gopinath [c]

[a] Department of Inorganic Chemistry, University of Madras, Guindy Campus, Chennai-600025, India
[b] Department of Chemistry, Vels Institute of Science, Technology & Advanced Studies, Pallavaram, 600117, Chennai, Tamil Nadu, India
[c] School of Bioprocess Engineering & Institute of Nano Electronic Engineering, Universiti Malaysia Perlis, 01000 Kangar, Perlis, Malaysia

ARTICLE INFO

Article history:
Received 15 September 2019
Revised 14 November 2019
Accepted 16 November 2019
Available online xxx

Keywords:
Nanoflakes
Pentoxifylline
Paracetamol, Electrochemical analysis
Urine samples

ABSTRACT

Simultaneous voltammetry determination of pentoxifylline (PTX) and paracetamol (PAR) were investigated by using graphene nanoflakes modified glassy carbon electrode (GrNF/GCE) in drug and biological samples. The synthesized flake was characterized using various analytical methods and the electron transfer behavior of GrNF was confirmed by CV and EIS techniques. Electrocatalytic oxidation of PTX and PAR at GrNF/GCE occurred at a potential of +1.220 V and + 0.190 V. The peak to peak separation (900 mV) was obtained for PTX and PAR at GrNF/GCE using DPV method. Amperometry technique was carried out to measure the current response of PTX and PAR and its dynamic ranges from 0.2×10^{-8}–300×10^{-6} M (0.9938) and 0.1×10^{-8}–150×10^{-6} M (0.9982). The LOD of PTX and PAR were determined to be 0.75 and 0.43 nM (S/N = 3), respectively. This system provides high-level sensitivity in the presence of an excess concentration of easily oxidizable interfering biological molecules and it shows a better reproducibility and repeatability. The present system has been effectively applied for the PTX and PAR determination in real samples.

1. Introduction

Pentoxifylline (PTX) is a methylxanthine derivative that can decrease the blood viscosity and enhance the blood flow in peripheral circulation, enhancing erythrocyte flexibility, diminishing fibrinogen concentration, protection against cancer and vascular claudication [1]. Through PTX, typically it is well tolerated at <1.2 g daily dosage, however, beyond this level cause as reported. Long-term usage of this drug is toxic and mutagenic such as headache, blurred vision, nausea, vomiting, diarrhea, chest pain, irregular heartbeat and red-pink urine [2]. Paracetamol (PAR) is used as analgesics and antipyretics which can reduce fever, body pain and also protection against ovarian cancer [3]. The Lethal dosage of PAR causes liver and kidney damage, skin rashes and inflammation of the pancreas. If alcohol consumption, it may lead to death [4]. Hence, it is important to estimate the PTX and PAR concentration in human urine samples. The colorimetry, electrophoresis, potentiometry, chromatography, fluorometry, electrochemical, high-performance liquid chromatography, densitometer, chemiluminescence and, spectrophotometry techniques have been testified for the estimation of PAR and PTX [5–15]. As above, the electrochemical technique is more successive and extensive due to their stability, selectivity, lower detection limit, wider linear range and, good repeatability.

Carbon materials (nanotubes, graphene, sphere, fiber, quantum dots, and carbon black) have a large surface area, easy to transfer electrons, high conductivity, extraordinary mechanical and thermal stability [16–20]. Newly, graphene materials [graphene nanodot (GrND), graphene nanoflake (GrNF), graphene nanoribbon (GrNR), graphene nanobelt (GrNB) and graphene membrane (GrMB)] are used as surface mediator owing to their current density and electron transfer property [21,22]. Among these, GrNF shows some edge defects which aid the rate of reaction and enhances the electrocatalytic ability for various electrochemical reactions [23]. The defect-free GrNF synthesized by the solvent exfoliation method has shown fast electron transport as well as excellent mechanical strength [24]. Recently, GrNF can be exploited for developing electrochemical sensors to detect some biologically important molecules and toxic pollutants [25–27].

We developed a novel voltammetric strategy for the simultaneous analysis of PTX and PAR in the presence of PTX derived

* Corresponding author.
E-mail address: jeevapandian@yahoo.co.uk (K. Pandian).

https://doi.org/10.1016/j.jtice.2019.11.011
1876-1070/

metabolites based on their oxidation using GrNF/GCE. Electrochemical impedance spectroscopy and cyclic voltammetry techniques were used to analyze the electron transfer behavior and GrNF/GCE surface defects. Simultaneous electrocatalytic oxidation of PTX and PAR shows a wider peak-potential window which confirmed by DPV technique. The advantage of the predictable work is simple and rapid and sensitive electrochemical determination of PTX and PAR in real samples at a minimal level. The interference effect of other PTX derived metabolites like xanthine and hypoxanthine are not affect the oxidative current density of PTX and PAR.

2. Experimental

2.1. Materials and reagents

Pentoxifylline and paracetamol were received from Hi-Media Chemicals Pvt. Ltd. (Sri Hari Scientific, Chennai, India). Potassium chloride, potassium nitrate, Trimethylhexacecyl ammonium bromide, dipotassium phosphate, potassium ferricyanide, and monopotassium phosphate were bought from Sisco Research Laboratories Pvt. Ltd., India. Graphite (powder, <20 µm, synthetic) was received from Bio corporals, Chennai. Acetone, ethanol, nitric acid and glacial acetic acid were obtained from CDH chemicals, Chennai. All tablets are collected from medical shops, Chennai, Tamilnadu.

The 0.1 M PTX and PAR stock solution was prepared using double distilled water and stored in a refrigerator at or below 4 °C until further use. Supporting electrolyte was prepared using a 500 mL standard flask by mixing 0.1 M of potassium chloride, dipotassium phosphate, and monopotassium phosphate. The redox probe was prepared by mixing 10 mM $[Fe(CN_6)]^{3-/4-}$ and 0.1 M KNO_3 using double distilled water.

2.2. Preparation of GrNF and modified GCE

To prepare GrNF [28], 50 mg graphite and 0.05 M trimethylhexacecyl ammonium bromide are taken in glacial acetic acid which was heated at 100 °C for 18 h. And then, the ensuing composite was centrifuged and washed three times using double distilled water, followed by acetone to get a stabilized GrNF. Approximately, 5 mg GrNF was mixed with 5 mL ethanol which was kept ultrasonic bath to obtain a uniform dispersion. The colloid suspension of GrNF (5 µL) was placed on the surface cleaned GCE (alumina paste followed by 1:1 *v/v* ratio of HNO_3 and acetone) and dried at room temperature.

2.3. Instruments

XPS experiment was carried out to study the elemental composition of GrNF using ESCA probe TPD spectrometer with Al Kα radiation (hυ = 1486.6 eV, Omicron nanotechnology). The surface functional groups were recorded using FT-IR spectrophotometer (Perkin-Elmer, model no. 360, USA) in the range 4000–400 cm^{-1} at a resolution of 4 cm^{-1}. Confocal Raman Spectroscopy was characterizing the GrNF using a Ne–Ar laser source of 532.9 nm wavelength with grating 600/mm (Model: 11I, Nanophoton, Japan). X-ray diffraction analysis was performed by Bruker (Model: D8 ADVANCE) with a Cu Kα Radiation (λ = 1.5406 Å). Structural morphology and chemical composition were recorded by scanning electron microscopy at the operating voltage 15.0 kV (model: SU6600, Hitachi, Japan) and energy dispersive X-ray analysis (EDX, 8121-H, Japan). Voltammetry and electrochemical impedance spectroscopy were measured the electron transfer property by Gamry and CH Instruments, USA. A three electrodes system consists of working (glassy carbon electrode), reference (Ag/AgCl) and counter electrodes (platinum wire) in a single cell setup. The surface area of the working electrode is 0.3 mm.

3. Results and discussion

3.1. Spectroscopy analysis of GrNF

The surface morphology of GrNF is predictable using scanning electron microscopic images. The shape of GrNF was regular as well as smooth flake structure and the typical size of flakes was found to be 30 nm with an operating voltage of 15.0 kV (Fig. 1(i)A and B.). The energy dispersive X-ray analysis (EDX) has recorded to measure the elemental composition of GrNF. From the EDX, carbon and, oxygen are the major elements present in GrNF as shown in *Fig. S1*. The surface functional groups of defect-free GrNF have been studied by FT-IR and Raman spectral studies. The FT-IR spectra of GrNF shows a higher absorption bands at 3418 and 1420 cm^{-1} corresponding COOH/O-H stretching vibration and alcoholic O-H (Fig. 1(ii)A) [29]. The absorption peak at 2923 cm^{-1} is associated with stretching vibration of the C-H group and a remaining bands at 1035, 1658 and 1743 cm^{-1} are owing to alkoxy carbonyl (C-O), stretching frequencies of C=C and C=O groups, respectively [30]. Fig. 1(ii)B exhibits graphite peaks at ~1355.52 cm^{-1} and ~1554.23 corresponds to the symmetry A_{1g} and first-order scattering E_{2g}. For GrNF, the D band at ~1332.01 cm^{-1} is Raman inactive and the new 2D band forms at ~2683.73 cm^{-1} that is the overtone of D band. Also, the signal is shifted towards lower wavenumbers due to the decrease in the number of layers. Additionally, the intensity ratio is estimated to be 0.87 and 1.08 for graphite and GrNF, which indicates a few-layered graphene sheet [31].

X-ray diffraction pattern of graphite depicts a sharp and intense peak at 26.40° with d-spacing value of 3.36 Å (Fig. 1(ii)C). The defect-free layers have been appeared at the peak intensity of 26° and 55° thereby indicating the formation of GrNF [32]. And also, the peak intensity has significantly decreased in the case of GrNF while compared to graphite. XPS spectrum was recorded for GrNF to studying the oxidation state and the binding nature of chemical constituents. The survey scan and individual elemental scan of XPS analysis are shown in Fig. 1(ii)D. The two major peaks were seen at 281.6 and 531.5 eV corresponds to the C 1 s and O 1 s signals, respectively. From the survey scan, it is inferred that the GrNF synthesized by this method has high purity and stable structure. The XPS data for GrNF is exactly matching with previously reported results [33].

3.2. Voltammetry analysis of GrNF

3.2.1. Electrochemical behavior of GrNF/GCE

Electrochemical property of GrNF/GCE was recorded using cyclic voltammetry in the occurrence of the redox probe with potential ranging from – 0.4 V to + 0.5 V vs. Ag/AgCl as shown in Fig. 2A. Based on the above observation, the bare GCE displays a peak potential separation (ΔE_p=E_{pa}-E_{pc}) between redox probe is 98 mV. Conversely, GrNF/GCE shows the potential difference (ΔE_p) of 63 mV (Nernstian value is 60 mV) and redox peak current ratio (I_{pa}/I_{pc}) is close to 1, henceforth representing the reaction is reversible and also GrNF/GCE shows large surface area and high conductivity as compared to bare GCE. In addition, the Randles-Sevick equation was utilized to measure the electroactive surface area (A) by;

$$I_p = 2.69 \times 10^5 A D^{1/2} n^{3/2} \upsilon^{1/2} C \quad (1)$$

where *D*, υ, *n*, *C*, I_p and *A* are the usual meaning of diffusion coefficient (redox probe equal to 0.76×10^{-6} cm^2 s^{-1}) [34], scan rate

Please cite this article as: S. Meenakshi, K. Pandian and S.C.B. Gopinath, Quantitative simultaneous determination of pentoxifylline and paracetamol in drug and biological samples at graphene nanoflakes modified electrode, Journal of the Taiwan Institute of Chemical Engineers, https://doi.org/10.1016/j.jtice.2019.11.011

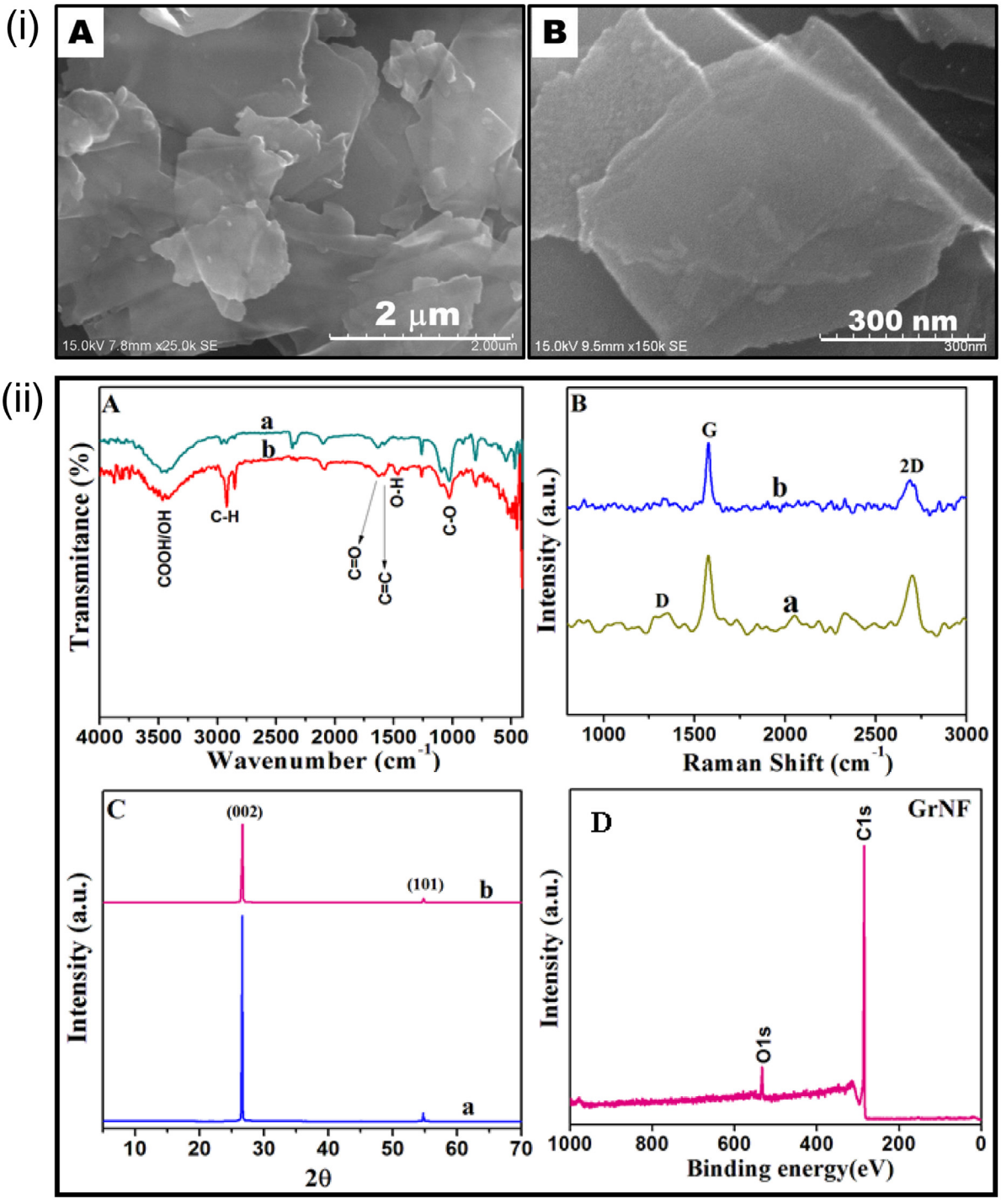

Fig. 1. (i) SEM images of GrNF (A and B) with an operating voltage of 15.0 kV. (ii) Surface analysis. (A) FT-IR spectra of (a) graphite and (b) GrNF, (B) Raman spectra of (a) graphite and (b) GrNF, (C) XRD pattern of (a) graphite and (b) GrNF and (D) XPS survey spectrum of GrNF.

(mVs^{-1}), number of electrons, redox peak current, concentration (mol cm^{-3}) and electroactive surface area (cm^2). Electroactive surface area is estimated to be 0.03 cm^2 and 0.076 cm^2 for bare GCE and GrNF/GCE thereby indicating the GrNF/GCE shows a large electrode surface, high conductivity, and excellent processability.

The influence of the potential scan rates of GrNF/GCE was examined by using redox probe as shown in *Fig. S2A*. The redox peaks displayed at a potential of +0.070 V and -0.010 V and peak current response increases while increasing sweep rates from 5–160 mV/s as well as linear relationship was obtained by plotting I_p against $\upsilon^{1/2}$. A linear regression equation of I_{pa} (μA) = 0.1790 ($\upsilon^{1/2}$/$mV^{1/2}/s^{1/2}$) + 0.0427 (0.9934) and I_{pc} = (μA) = -0.1665 ($\upsilon^{1/2}$/$mV^{1/2}/s^{1/2}$) - 0.1517 (0.9922), respectively (Fig. *S2B*), indicating the process of GrNF/GCE is purely diffusion-controlled one.

Nyquist plot of GrNF/GCE was investigated by EIS in the presence of a redox probe with frequency ranging from 0.01 Hz to 100,000 Hz (Fig. 2B). In bare GCE, a straight line appeared resulting in the process is diffusion-limited. The GrNF/GCE exhibits a slight semicircle which demonstrates that the redox reaction is diffusion-

Please cite this article as: S. Meenakshi, K. Pandian and S.C.B. Gopinath, Quantitative simultaneous determination of pentoxifylline and paracetamol in drug and biological samples at graphene nanoflakes modified electrode, Journal of the Taiwan Institute of Chemical Engineers, https://doi.org/10.1016/j.jtice.2019.11.011

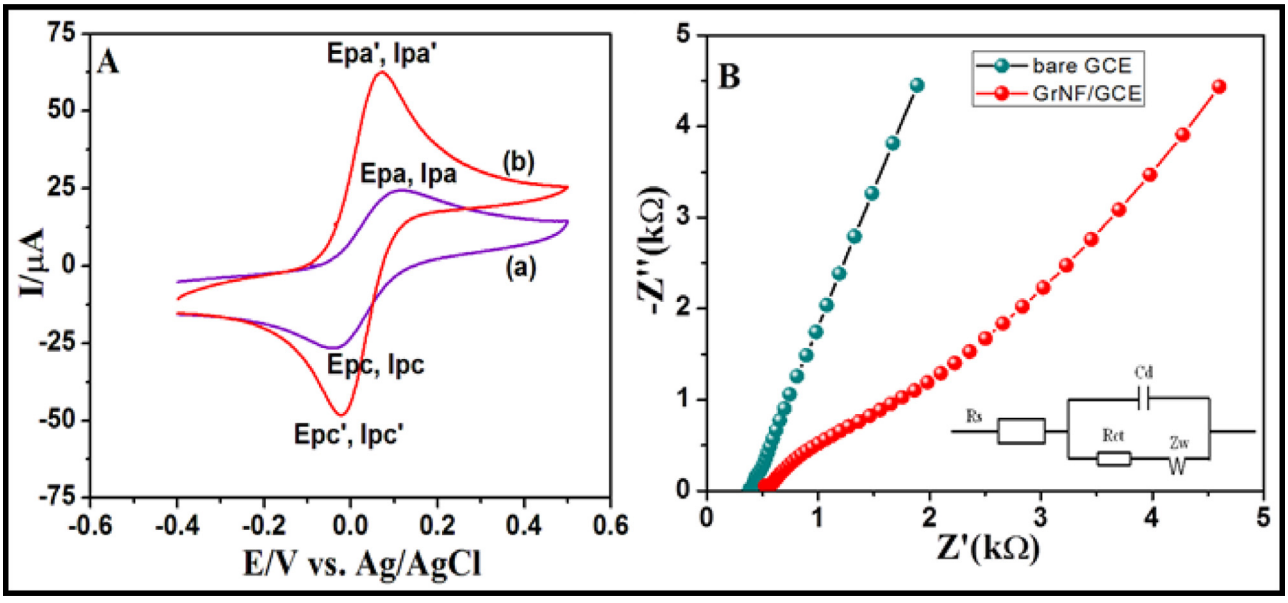

Fig. 2. (A) CV of (a) bare GCE and (b) GrNF/GCE in a solution containing 10 mM $[Fe(CN)_6]^{3-/4-}$ and 0.1 M KNO_3 at a scan rate of 50 mV/s. (B) Nyquist plots of bare GCE and GrNF/GCE in a solution containing 10 mM $[Fe(CN)_6]^{3-/4-}$ and 0.1 M KNO_3. AC Amplitude: 5 mV; Frequency range: 0.01 Hz to 100 kHz. Inset is the Randles circuit.

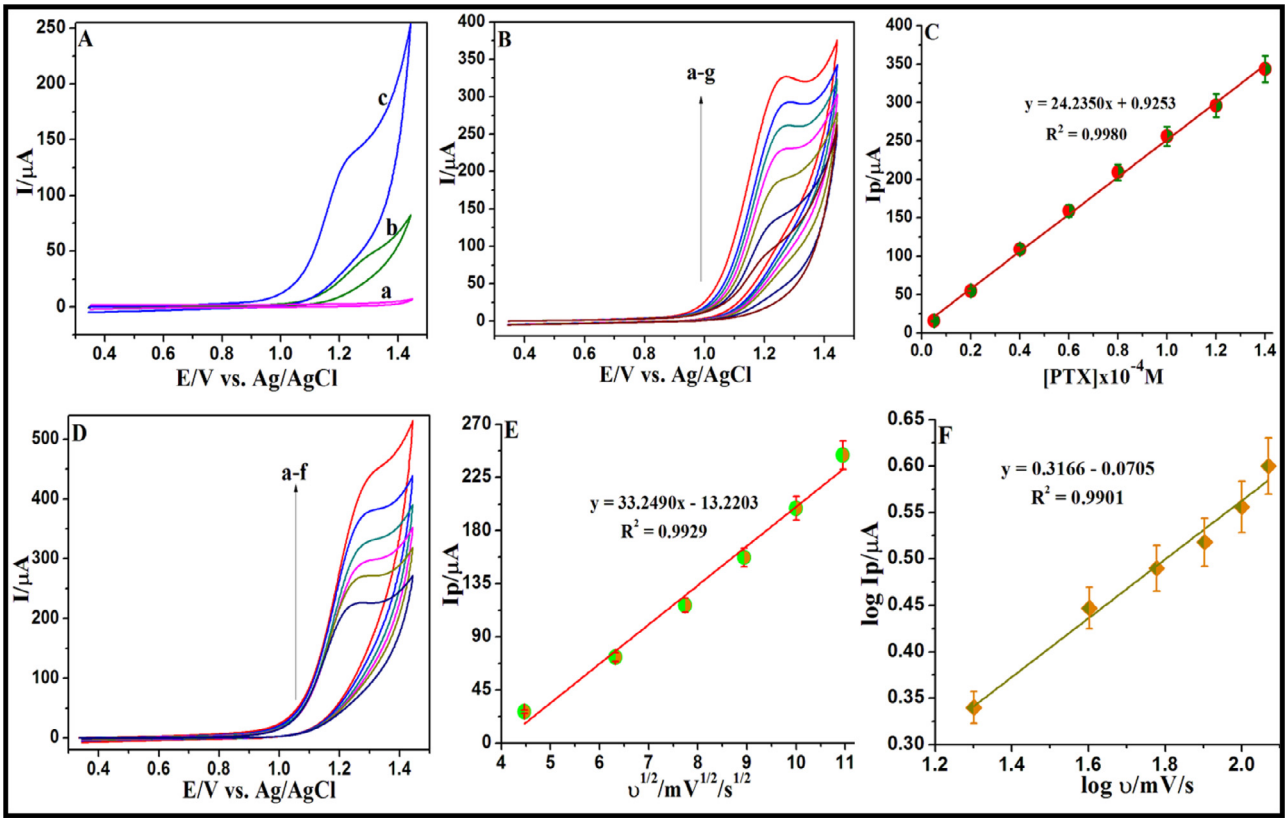

Fig. 3. (A) CV of a) and b) bare GCE (absence and presence of PTX) and c) GrNF/GCE in the presence of 0.1 mM of PTX at a scan rate 50 mV/s in 0.1 M KCl containing PBS (pH 7.0). (B) CV of GrNF/GCE in different concentrations (0.2 to 1.4×10^{-4} M) of PTX at a scan rate of 50 mV/s (a–g). (C) Calibration plot of I_{pa} vs. conc. of PTX. (D) CV of GrNF/GCE in presence of 0.1 mM PTX at various scan rates from 20−120 mV/s (a-f). (E) Plot of I_{pa} vs. $\upsilon^{1/2}$. (F) Logarithmic plot of I_{pa} vs. υ.

controlled one [35]. Hence, the proposed material is considered for the electrochemical analysis of drug and biological samples.

3.2.2. Electrocatalytic property of PTX at GrNF/GCE

Electrocatalytic activity of PTX was tested in the occurrence of 0.1 M KCl containing phosphate buffer solution (PBS) at pH 7.0 and the resulting behavior as shown in Fig. 3A. PTX exhibits poor anodic current with a potential (E_{pa}) + 1.290 V at bare GCE whereas, the modified system reveals high current density and the peak potential (E_{pa}) at + 1.230 V. While increasing the concentration of PTX from 0.2 to 1.4×10^{-4} M, the peak increases linearly as indicated in Fig. 3B and C [36]. The influence of scan rate was per-

Please cite this article as: S. Meenakshi, K. Pandian and S.C.B. Gopinath, Quantitative simultaneous determination of pentoxifylline and paracetamol in drug and biological samples at graphene nanoflakes modified electrode, Journal of the Taiwan Institute of Chemical Engineers, https://doi.org/10.1016/j.jtice.2019.11.011

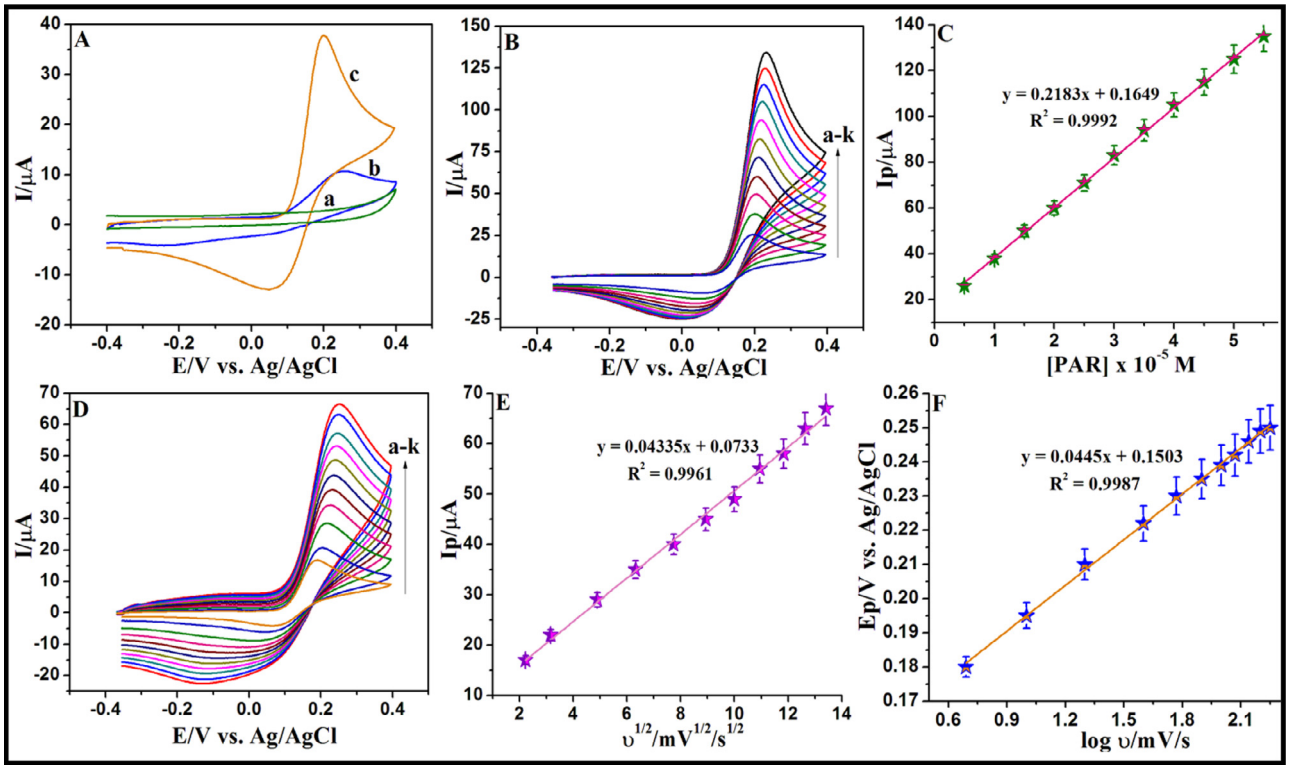

Fig. 4. (A) CV of a) and b) bare GCE (absence and presence of PAR) and c) GrNF/GCE in the presence of 0.1 mM PAR at a scan rate of 50 mV/s in 0.1 M KCl containing PBS (pH 7.0). (B) CV of GrNF/GCE in different concentrations (0.5 to 5.5×10^{-5} M) of PAR at a scan rate of 50 mV/s (a–k). (C) Calibration plot of I_{pa} vs. conc. of PAR. (D) CV of GrNF/GCE in presence of 0.1 mM PAR at various scan rates from 5 to 180 mV/s (a-k). (E) Plot of I_{pa} vs. $\upsilon^{1/2}$. (F) Plot of E_{pa} vs. log υ.

formed using GrNF/GCE towards PTX. The scan rate ranging from 20 - 120 mV s^{-1}, the oxidative current response enlarge linearly and a shift in E_{pa} at positive direction was detected (Fig. 3*D*). A straight line can be obtained from I_{pa} against $\upsilon^{1/2}$, resulting a linear regression equation of I_{pa} (μA) = 33.2490 $\upsilon^{1/2}$ ($mV^{1/2}/s^{1/2}$) -13.2203 (0.9929) (Fig. 3*E*). These results indicating the electron transfer process is diffusion-controlled towards the oxidation of PTX. Additionally, the surface concentration (Γ) of PTX was calculated using the slope of I_p-$\upsilon^{1/2}$ in Fig. 3E [37] corresponds to;

$$I_p = n^2F^2\Gamma A\upsilon/4RT \quad (2)$$

where I_p, n, F, υ, R and T are the usual meaning of peak current (μA), number of electrons, Faraday constant (C mol^{-1}), scan rate (mVs^{-1}), gas constant (J K^{-1} mol^{-1}) and temperature. Using the above equation, the Γ value of PTX was calculated to be 6.06×10^{-7} mol cm^{-2} at GrNF/GCE, which depicts the reaction process is a diffusion-controlled one. Furthermore, a straight line was detected with logarithmic peak current versus logarithmic scan rate (Fig. 3F), according to [38];

$$\log I_p/\mu A = 0.3166 \log \upsilon/mV/s - 0.0705;\ (R^2) = 0.9901 \quad (3)$$

The slope value is equal to theoretical value depicting the diffusion-controlled electrochemical oxidative process of PTX.

3.2.3. Electrocatalytic property of PAR at GrNF/GCE

Electrocatalytic performance of GrNF/GCE was studied towards the oxidation of PAR at GrNF/GCE as shown in Fig. 4A. PAR exhibits deprived redox current at a potential (E_{pa} and E_{pc}) of +0.254 V and −0.243 V for bare GCE whereas, the modified system exhibits a clear sharp potential (E_{pa} and E_{pc}) at +0.19 V and + 0.068 V, suggesting the electrocatalytic behavior of PAR is a quasi-reversible one. Even though, the oxidative peak current of PAR at GrNF/GCE is greater than unmodified GCE. A straight line was observed while increased the concentration (0.5 to 5.5×10^{-5} M), thereby indicating the excellent electrochemical performance of GrNF/GCE towards PAR (Fig. 4B and C). The effect of potential scan rates was studied against peak current of PAR, with increasing potential scan rates from 5–180 mV s^{-1}, the E_{pa} shifts to a positive direction and I_{pa} increases gradually (Fig. 4*D*). A straight line can be attained for the I_{pa} versus $\upsilon^{1/2}$, resulting in the PAR oxidation at GrNF/GCE is a diffusion-controlled process (Fig. 4*E*). The calculated Γ value of PAR using the slope of I_p vs. $\upsilon^{1/2}$ (Fig. 4*E*) was found to be 1.69×10^{-8} mol cm^{-2} at GrNF/GCE, which confirms that the reaction is purely diffusion-controlled one. Also, the PAR peak current increases linearly and the E_{pa} value shifted positively, designates that kinetic limitation in the electrochemical reaction. And, the E_{pa} has a linear relationship with log υ (Fig. 4F), which follows [39];

$$\log k_s = a\log(1-a) + (1-a)\log a - \log RT/nF\upsilon - a(1-a)n\,FDE_p/2.3\,RT \quad (4)$$

where k_s, R, F, T, υ, α and n are the usual meaning of standard heterogeneous reaction rate constant (s^{-1}), universal gas constant (J K^{-1} mol^{-1}), Faraday constant (C mol^{-1}), absolute temperature, scan rate (mV s^{-1}), electron transfer coefficient and number of electrons. Use that Eq. (4), the value of α, n and, k_s are predicted to be 0.48, 2.01 and 2.05 s^{-1}.

3.3. Influence of pH effect on PTX and PAR oxidation

The influence of pH effect was investigated against I_{pa} and E_{pa} of PTX and PAR oxidation at GrNF/GCE. It can be observed from Fig. 5A and B, the peak current and potential shift were noticed

Please cite this article as: S. Meenakshi, K. Pandian and S.C.B. Gopinath, Quantitative simultaneous determination of pentoxifylline and paracetamol in drug and biological samples at graphene nanoflakes modified electrode, Journal of the Taiwan Institute of Chemical Engineers, https://doi.org/10.1016/j.jtice.2019.11.011

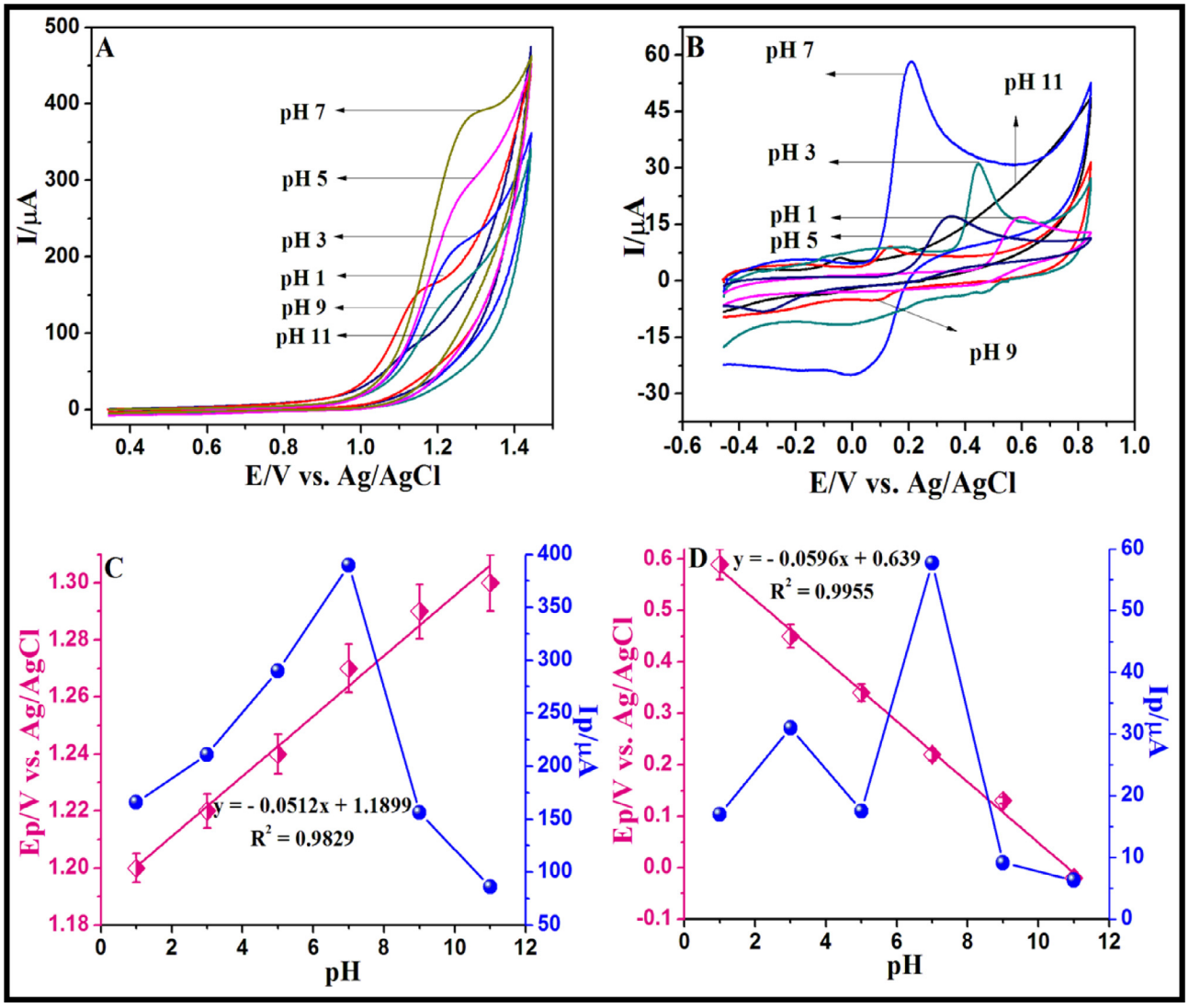

Fig. 5. Effect of pH on (A and B) CV curves of 0.1 mM of PTX and PAR at GrNF/GCE in the presence of 0.1 M KCl containing PBS with various pH ranges (pH 1, 3, 5, 7, 9 and 11) at a scan rate of 50 mV/s. (C) Effect of pH on E_{pa} and I_{pa} of PTX. (D) Effect of pH on E_{pa} and I_{pa} of PAR.

for both PTX and PAR while enhancing the pH of the medium and the maximum I_{pa} was seen at pH 7.0. The slope value 59.6 and 51.2 mV pH^{-1} represent that the reaction involves an equal number of protons/electrons participated in the electrochemical oxidation of both PAR and PTX (Fig. 5C and D) at GrNF/GCE [36,40,41]. The mechanistic steps of PTX and PAR at GrNF/GCE are shown in *Fig. S3.*

3.4. Chronoamperometry method for PAR at GrNF/GCE

The diffusion coefficient of PAR at GrNF/GCE was determined by Chronoamperometric technique at the working potential of + 0.2 V as a resulting plot shown in Fig. 6A. The diffusion coefficient was estimated using the following equation with the slope value of I_p versus $t^{-1/2}$ (Fig. 6B) [42].

$$I = nFACD^{1/2}\pi^{-1/2}t^{-1/2} \quad (5)$$

where *n, C, D, F* and *A* are the number of electrons participated in PAR oxidation, the bulk concentration of an analyte (mol cm^{-3}), diffusion coefficient (cm^2 s^{-1}), Faraday constant (C mol^{-1}) and electrode area (cm^2). The *D* was estimated to be 7.54×10^{-6} cm^2 s^{-1} which depicting the enhanced electrocatalytic oxidation of PAR occurs at GrNF/GCE.

3.5. Sensitivity dependence of PTX and PAR at GrNF/GCE

PTX and PAR drugs are administered to cure some diseases. In that case, the proposed method can be extending to the detection of both analytes simultaneous using this electrochemical method. By keeping this idea in mind, a linear sweep voltammogram is recorded to observe the voltammetric behavior of both PTX and PAR in presence of other PTX derived metabolites like xanthine and hypoxanthine as major derivatives of PTX and the resulting LSV behavior of the molecules are shown Fig. S4 and a well-defined oxidation peak observed for all individual molecules. However, LSV cannot be used for the quantitative detection at lower concentration ranges in biological samples because of its poor sensitivity. The sensitive oxidation of PTX and PAR at GrNF/GCE was noticed at the same time by DPV technique in 0.1 M KCl in PBS (pH 7.0). In simultaneous determination, the concentration of PTX increases and the PAR kept as a constant and vice-versa as shown in Fig. 7, under optimal experimental condition.

Please cite this article as: S. Meenakshi, K. Pandian and S.C.B. Gopinath, Quantitative simultaneous determination of pentoxifylline and paracetamol in drug and biological samples at graphene nanoflakes modified electrode, Journal of the Taiwan Institute of Chemical Engineers, https://doi.org/10.1016/j.jtice.2019.11.011

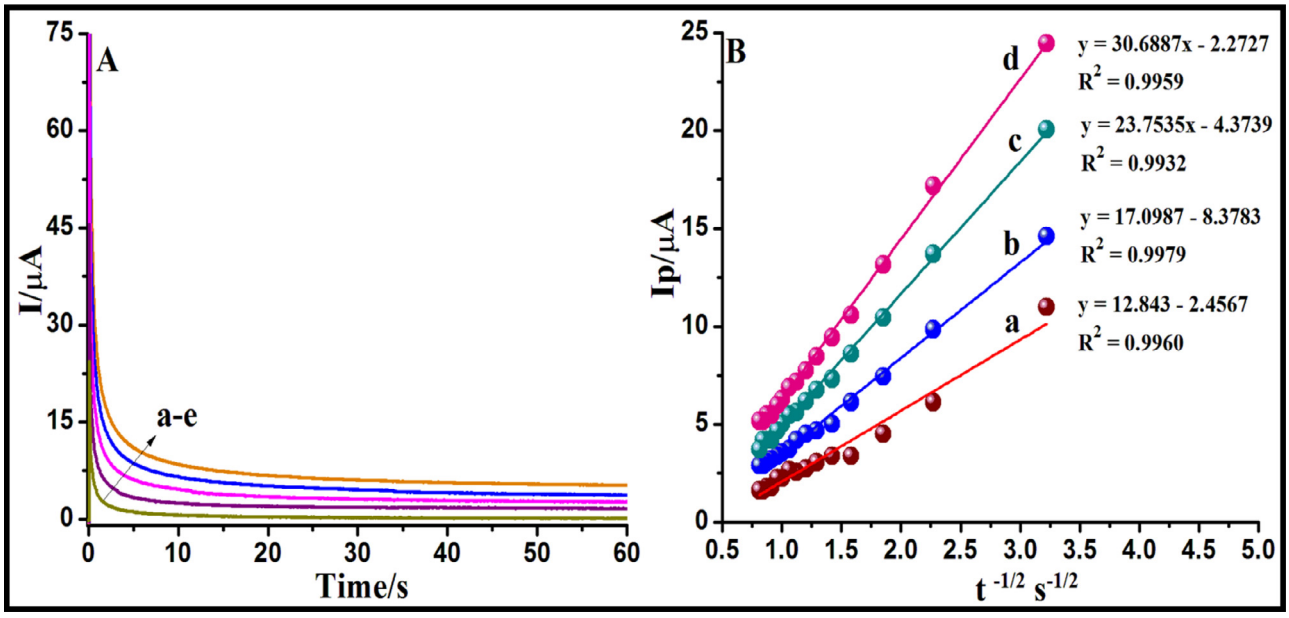

Fig. 6. (A) CA obtained at GrNF/GCE in the absence and presence of (0.05 to 0.2 mM) of PAR in 0.1 M KCl containing PBS (pH 7.0) at the potential step of 200 mV. (B) Cottrell plots drawn using data obtained from CA b) to e) from (A).

As can be observed from Fig. 7A and C, the concentration of PTX and PAR were increased linearly, the E_p of PTX and PAR at +1.05 and +0.15 V as remained constant. The peak-to-peak separation of both PTX and PAR at GrNF/GCE can be predicted to be 900 mV and the linear dynamic ranging from 0.5 – 5.5×10^{-8} M and 1 – 13×10^{-8} M for PTX and PAR. Fig. 7B and D shows the linear regression equation of PTX and PAR are I_{pa} (μA) = 0.8181 (10^{-8} M) + 0.584 ($R^2 = 0.9906$) and I_{pa} (μA) = 2.2859 (10^{-8} M) + 0.0157 ($R^2 = 0.9987$) with the detection limit of 4.5 and 3.6 nM, respectively. Table S1 shows the comparison of proposed and previous literature detection limits of PAR and the PTX detection limit is lower than MWCNTPE [43] and GCE [44]. Based on the above observation, the electrochemical determination of both PTX and PAR displays high sensitivity, wider potential window and lower limit of detection.

3.6. Amperometry detection of PTX and PAR at GrNF/GCE

The peak current response of PTX and PAR at GrNF/GCE can be easily measured by using amperometric technique with respective time interval and an applied potential + 1.05 and 0.2 V. The catalytic current-time response of PTX and PAR reveals a linear increase of I_p with respective concentration at every 50 s as shown in Figure S5A and C. In amperometry studies, a linear peak current increases with increasing analytes concentration ranging from 0.2 – 3×10^{-8} M for PTX and 0.1 – 1.5×10^{-8} M for PAR with a detection limit of 0.75 nM (0.9938) and 0.43 nM (0.9982), respectively. The sensitivity of PTX and PAR were calculated to 10.71 μA nM^{-1} cm^{-2} and 6.14 μA nM^{-1} cm^{-2} (*Fig. S5B and D*), thereby indicating a better sensitivity against GrNF/GCE towards PTX and PAR oxidation.

3.7. High-performance studies

The storage and long-term stability of GrNF/GCE were examined and used to store the refrigerator around 40°F. Later than 15 days, to check the peak current response of GrNF/GCE and has maintained 99.3% than freshly made. Again to check the response after 30 days, the current retained at 98.5%, this by suggestive of GrNF/GCE reveals better stability. The reproducibility of the generated sensor was detected by using the amperometry method at different time intervals. The current response has conserved similar to R. S. D value ±3.3% ($n = 5$), which suggests that reproducibility and stability is superior at GrNF/GCE system.

3.8. Interference studies

Many substances have potentially interfered with electrochemical oxidation of PTX and PAR in the occurrence of 0.1 M KCl containing PBS (pH 7.0). The chosen of interference species has scrutinized against the oxidation of PTX and PAR at GrNF/GCE. The present system obtained no interference for the detection of PAR and PTX, such species are uric acid (UA), theophylline, guanine, adenine, aspirin, caffeine, folic acid, tyrosine, tryptophan, ascorbic acid (AA), Na^+, Fe^{2+} and dopamine (DA) as shown in Fig. S6. Based on the observation, the species have not interfered with PTX and PAR determination up to a minimum of 50-fold excess.

3.9. Real sample analysis

3.9.1. PTX and PAR determination in pharmaceuticals

DPV technique was used to analyze the PTX and PAR determination in tablet samples. Tablet samples were accurately weighed and finely ground in a mortar. A chosen amount of powder sample was dissolved by using sonicater and then taken a different quantity of prepared solution has mixed with phosphate buffer solution. After that, a cell containing 15 mL of prepared solution and the current response was noticed. The results were summarized and listed in Table S2. These results demonstrated that GrNF/GCE electrochemical sensing platform held great promise for reliable and sensitive applications in clinical analysis.

3.9.2. PTX estimations in human urine samples

In human urine samples, the concentration of PTX can be tested by amperometric technique. All the urine samples were received by Adyar Cancer Hospital, Chennai and diluted 200 times with 0.1 M PBS at pH 7.0. After that, a cell with 15 mL of a prepared urine sample and a certain amount PTX was injected and the current response was notified. The recovery range and R.S.D ($n = 5$)

Please cite this article as: S. Meenakshi, K. Pandian and S.C.B. Gopinath, Quantitative simultaneous determination of pentoxifylline and paracetamol in drug and biological samples at graphene nanoflakes modified electrode, Journal of the Taiwan Institute of Chemical Engineers, https://doi.org/10.1016/j.jtice.2019.11.011

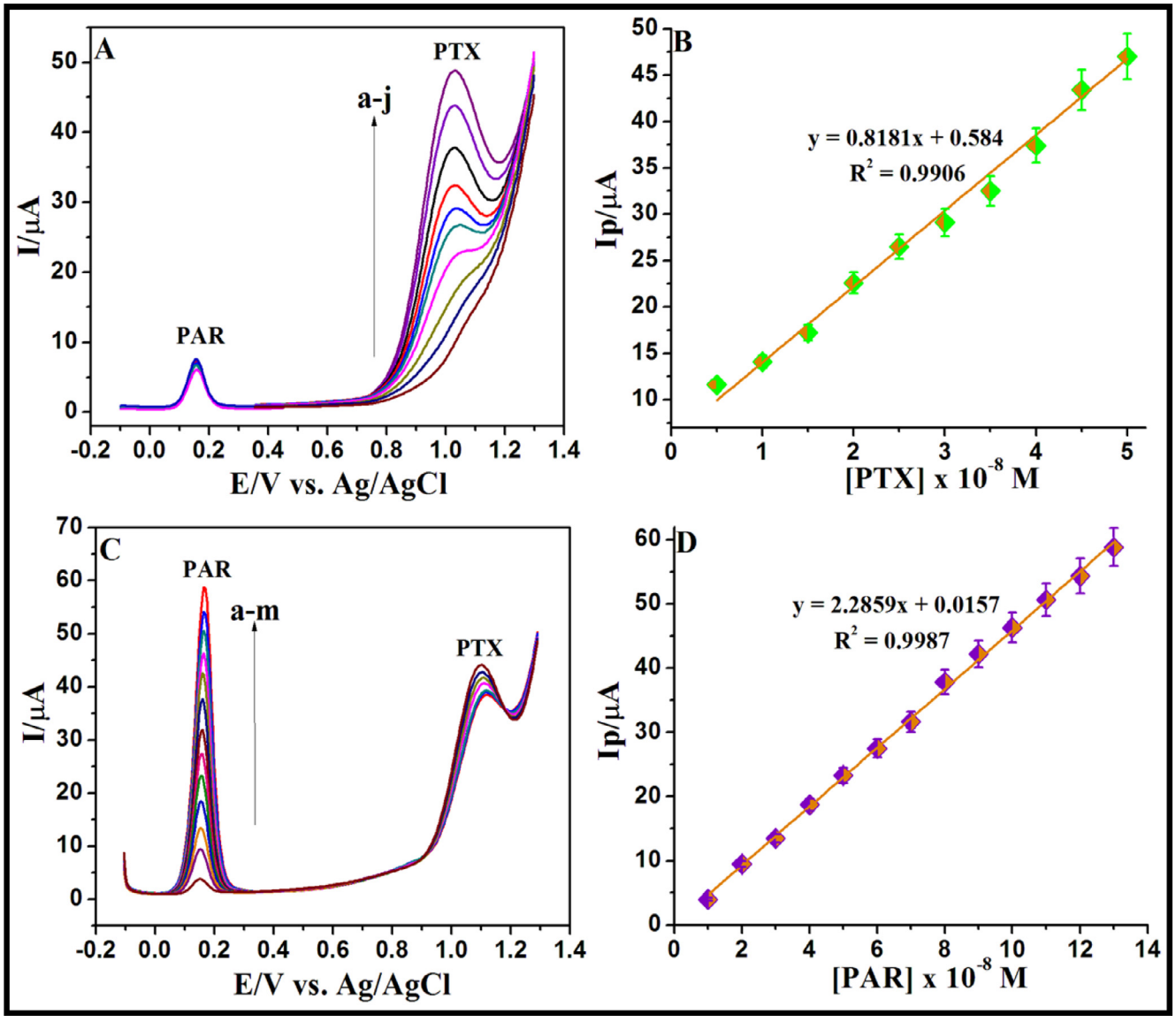

Fig. 7. (A) DPV of PTX at GrNF/GCE in 0.1 M KCl containing PBS (pH 7.0) in presence of 50 μM PAR (0.5×10^{-8} M–5.5×10^{-8} M from a–j). (B) Plot of I_{pa} vs. conc. of PTX. (C) DPV of PAR at GrNF/GCE in 0.1 M KCl containing PBS (pH 7.0) in presence of 50 μM PTX (1×10^{-8} M–13×10^{-8} M from a–m). (D) Plot of I_{pa} vs. conc. of PAR. Scan rate: 20 mV/s, Pulse width: 50 mV, Pulse Amplitude: 25 mV.

value of PTX are listed in *Table S3*, suggesting the modified electrode shows good reliability and repeatability towards PTX determination in human samples.

4. Conclusion

A sensitive and novel method for the estimation of PTX and PAR at GrNF/GCE was analyzed. The proposed system exhibited a simultaneous detection against PTX and PAR which suggests good electrocatalytic activity and a well-defined peak potential separation. Additionally, the preparation of GrNF/GCE reveals simple and easier than all previously reported studies. Thus, the most important issue to estimation the concentration of PTX and PAR directly in drug and human urine samples, so the goal of this study was to estimate the simultaneous determination of PTX and PAR in real samples. GrNF/GCE was found to be a potentially valuable tool for designing a well-organized and tremendously selective electrochemical sensor for PTX and PAR in real samples at trace level.

Declaration of Competing Interest

The authors declare that they have no known competing financial interests or personal relationships that could have appeared to influence the work reported in this paper.

Acknowledgment

We thank DST (Department of Science and Technology DST-SERB programme EEQ/2016/00733), New Delhi and National Centre for Nanoscience and Nanotechnology, University of Madras.

Supplementary material

Supplementary material associated with this article can be found, in the online version, at doi:10.1016/j.jtice.2019.11.011.

Please cite this article as: S. Meenakshi, K. Pandian and S.C.B. Gopinath, Quantitative simultaneous determination of pentoxifylline and paracetamol in drug and biological samples at graphene nanoflakes modified electrode, Journal of the Taiwan Institute of Chemical Engineers, https://doi.org/10.1016/j.jtice.2019.11.011

References

[1] Aiman U, Haseen MA, Beg MH, Khan RA, Siddiqui FA, Alam I. Profile of atherosclerotic risk factors and management in patients of peripheral arterial disease at a tertiary care teaching hospital of north India. Indian J Pharm Sci 2014;76:504–9.
[2] Samir KP, Michael PD, James HS, Matthias AC, Ziyue L. A pilot trial of pentoxifylline on endothelial function and inflammation in HIV-infected patients initiating antiretroviral therapy. AIDS 2016;30:2139–42.
[3] Roofthooft DWE, Simons SHP, Vanlingen RA, Tibboel D, Anker JNVd, Reiss IKH. Randomized controlled trial comparing different single doses of intravenous paracetamol for placement of peripherally inserted central catheters in preterm infants. Neonatology 2017;112:150–8.
[4] Batema DN, Carroll R. Effect of the UK's revised paracetamol poisoning management guidelines on admissions, adverse reactions and cost of the treatment. Br J Clin Pharmacol 2014;78:610–18.
[5] Ellcock CTH, Fogg AG. Selective colorimetric determination of paracetamol by means of an indophenol reaction. Analyst 1975;1186:16–18.
[6] Wirat R, Saisunee L, Alan T. Flow injection chemiluminescence determination of paracetamol. Talanta 2006;69:976–83.
[7] Borahan T, Unutkan T, Sahin A, Bakiradere S. A rapid and sensitive reversed phase-HPLC method for simultaneous determination of ibuprofen and paracetamol in drug samples and their behaviors in simulated gastric conditions. J Sep Sci 2019;42:678–83.
[8] Mostafa NM. Stability indicating method for the determination of paracetamol in its pharmaceutical preparations by tlc densitometric method. J Saudi Chem Soc 2010;14:341–4.
[9] Khoobi A, Attaran AM, Yousofi M, Enhessari M. A sensitive lead titanate nano-structured sensor for electrochemical determination of pentoxifylline drug in real samples. J Nanostruct Chem 2019;9:29–37.
[10] Pandian K, Bindu U, Narayanan S. Indirect potentiometric determination of pentoxifylline in pharmaceutical preparations. Pharmazie 1993;48:621–2.
[11] Ashraf MM, Saad AAQ. Spectrophotometric study for the reaction of pentoxifylline hydrochloride with 1,2-naphthoquinone-4-sulphonate: kinetics, mechanism and application for development of high-throughput kinetic microwell assay for pentoxifylline in quality control laboratory. Am J Anal Chem 2016;7:179–91.
[12] Mohamed AK, Rim SH, Marwa AAR, Osama AE. Kinetic investigation of pentoxifylline based on nonparametric linear regression derivative and convoluted derivative chromatographic and spectrophotometric responses. J Liquid Chromatogr Relat Technol 2014;37:475–97.
[13] Kishan SL, Saurabh S, Ishit K, Deepak C, Anupama M. Simultaneous estimation of lisofylline and pentoxifylline in rat plasma by high performance liquid chromatography – photodiode array detector and its application to pharmacokinetics in rat. J Chromatogr B 2017;1061-1062:49–56.
[14] Kalaiyarasi J, Meenakshi S, Gopinath SCB, Pandian K. Mediator-free simultaneous determination of acetaminophen and caffeine using a glassy carbon electrode modified with a nanotubular clay. Microchim Acta 2017;184:4485–94.
[15] Rafael RC, Sandro CC, Michelle MACR, Livia MFCT, Rodrigo AAM, Wallans TPDS. Simultaneous determination of caffeine, paracetamol, and ibuprofen in pharmaceutical formulations by high-performance liquid chromatography with UV detection and by capillary electrophoresis with conductivity detection. J Sep Sci 2015;38:1657–62.
[16] Yang C, Denno ME, Pyakurel P, Venton BJ. Recent trends in carbon nanomaterial-based electrochemical sensors for biomolecules. Anal Chim Acta 2015;887:17–37.
[17] Mao X, Rutledge GC, Hatton TA. Nanocarbon based electrochemical systems for sensing, electrocatalysis and energy storage. Nano Today 2014;9:405–32.
[18] Li X, Tao Y, Li F, Huang M. Efficient preparation and characterization of graphene with versatile applicability. J Harbin Inst Technol (New Ser) 2016;23:1–29.
[19] E.A. Arkhipova, A.S. Ivanov, K.I. Maslakov, A.V. Egorov, S.V. Savilov, V.V. Lunin, Mesoporous graphene nanoflakes for high performance supercapacitors with ionic liquid electrolyte, microporous and mesoporous materials, (2019) doi:10.1016/j.micromeso.2019.109851.
[20] Avouris P, Dimitrakopoulos C. Graphene: synthesis and applications. Mater Today 2012;15:86–97.
[21] Omidvar A, Mohajeri A. Edge functionalized graphene nanoflakes as selective gas sensors. Sens Actuat B 2014;202:622–30.
[22] Martin A, Ferrer JH, Martinez MT, Escarpa A. Graphene nanoribbion based electrochemical sensors on screen-printed platforms. Electrochim Acta 2015;172:2–6.
[23] Legrand U, Meunier JL, Berk D. Iron functionalized on graphene nanoflakes using thermal plasma for catalytic applications. Appl Catal A 2016;528:36–43.
[24] Wu C, Cheng Q, Wu K, Wu G, Li Q. Graphene prepared by one pot solvent exfoliation as a highly sensitive platform for electrochemical sensing. Anal Chim Acta 2014;825:26–33.
[25] Yang X, Long J, Sun D. Highly-sensitive electrochemical determination of rutin using NMP-exfoliated graphene nanosheets modified electrode. Electroanalysis 2016;28:83–7.
[26] Meenakshi S, Jancy Shopia S, Pandian K. High surface graphene nanoflakes as sensitive sensing platform for simultaneous electrochemical detection of metronidazole and chloramphenicol. Mater Sci Eng C 2018;90:407–19.
[27] Mutyala S, Mathiyarasu J. Preparation of graphene nanoflakes and its application for detection of hydrazine. Sens Actuat B 2015;210:692–9.
[28] Kalaiyarasi J, Meenakshi S, Pandian K, Gopinath SCB. Simultaneous voltammetric determination of vanillin and guaiacol in food products on defect free graphene nanoflakes modified glassy carbon electrode. Microchim Acta 2017;162:1–10.
[29] Yoon OJ, Kim I, Sohn IY, Kieu TT, Lee NE. Toxicity of graphene nanoflakes evaluated by cell based electrochemical impedance biosensing. J Biomed Mater Res 2014;102A:2288–94.
[30] Yoon OJ, Kim CH, Sohn IY, Lee NE. Toxicity analysis of graphene nanoflakes by cell based electrochemical sensing using an electrode modified with nanocomposite of graphene and nafion. Sens Actuat B 2013;188:451–61.
[31] Liu HW, Hu SH, Chen YW, Chen SY. Characterization and drug release behavior of highly responsive chip-like electrically modulated reduced graphene oxide-poly (vinyl alcohol) membranes. J Mater Chem 2012;22:17311–20.
[32] Allen MJ, Tung VC, Kaner RB. Honeycomb carbon: a review of graphene. Chem Rev 2010;110:132–45.
[33] B.D. Ossonon, D. Belanger, Functionalization of graphene sheets by the diazonium chemistry during electrochemical exfoliation of graphite, Carbon 111 (2017) 83–93.
[34] Lu W, Liu S, Qin X, Wang L, Tian J, Luo Y. High yield, large scale production of few layer graphene flakes within seconds: using chlorosulfonic acid and H_2O_2 as exfoliating agents. J Mater Chem 2012;22:8775–7.
[35] Laviron E. General expression of the linear potential sweep voltammogram in the case of diffusionless electrochemical systems. J. Electroanal Chem 1979;101:19–28.
[36] Meenakshi S, Devi S, Pandian K, Devendiran R, Selvaraj P. Sunlight assisted synthesis of silver nanoparticles in zeolite matrix and study of its application on electrochemical detection of dopamine and uric acid in urine samples. Mater Sci Eng, C 2016;69:85–94.
[37] El-Bouabi Y, Farahi A, Achak M, Zeroual M, Hnini K, El-Houssame S, Bakasse M. Electrocatalytic effect of fluoroapatite in reducing paracetamol at carbon paste electrode: analytical application. J. Taiwan Inst Chem Eng 2016;66:33–42.
[38] Bard AJ, Faulkner LR. Electrochemical methods: fundamentals and applications. 2nd ed. New York: Wiley; 2001.
[39] Hegde RN, Hosamani RR, Nandibewoor ST. Electrochemical oxidation and determination of theophylline at a carbon paste electrode using cetyltrimethyl ammonium bromide as enhancing agent. Anal Lett 2009;42:2665–82.
[40] Laviron E. General expression of the linear potential sweep voltammogram in the case of diffusionless electrochemical systems. J Electroanal Chem 1979;101:19–28.
[41] Pandian K, Bindu U, Suresh KPO, Narayanan SS. Indirect determination of pentoxifylline in drug formulations by biamperometry. Bull Electrochem 1993;9:127–9.
[42] Denuault G, Mirkin MV, Bard AJ. Direct determination of diffusion coefficients by chronoamperometry at microdisk electrodes. J Electroanal Chem 1991;308:27–38.
[43] Abbar JC, Malode SJ, Nandibewoor ST. Electrochemical determination of a hemorhelogic drug, pentoxifylline at a multi-walled carbon nanotube paste electrode. Bioelectrochemistry 2012;83:1–7.
[44] Hegde RN, Nandibewoor ST. Electrochemical oxidation of pentoxifylline and its analysis in pure and pharmaceutical formulations at a glassy carbon electrode. Anal Lett 2008;41:977–91.

Please cite this article as: S. Meenakshi, K. Pandian and S.C.B. Gopinath, Quantitative simultaneous determination of pentoxifylline and paracetamol in drug and biological samples at graphene nanoflakes modified electrode, Journal of the Taiwan Institute of Chemical Engineers, https://doi.org/10.1016/j.jtice.2019.11.011